SUMOylation of the MAGUK protein CASK regulates dendritic spinogenesis

Hsu-Wen Chao,[1,2] Chen-Jei Hong,[1,2] Tzyy-Nan Huang,[1,2] Yi-Ling Lin,[2,3] and Yi-Ping Hsueh[1,2,3]

[1]Graduate Institute of Life Science, National Defense Medical Center, [2]Institute of Molecular Biology, Academia Sinica, and [3]Graduate Institute of Genome Sciences, National Yang-Ming University, Taipei 11529, Taiwan

Membrane-associated guanylate kinase (MAGUK) proteins interact with several synaptogenesis-triggering adhesion molecules. However, direct evidence for the involvement of MAGUK proteins in synapse formation is lacking. In this study, we investigate the function of calcium/calmodulin-dependent serine protein kinase (CASK), a MAGUK protein, in dendritic spine formation by RNA interference. Knockdown of CASK in cultured hippocampal neurons reduces spine density and shrinks dendritic spines. Our analysis of the time course of RNA interference and CASK overexpression experiments further suggests that CASK stabilizes or maintains spine morphology. Experiments using only the CASK PDZ domain or a mutant lacking the protein 4.1–binding site indicate an involvement of CASK in linking transmembrane adhesion molecules and the actin cytoskeleton. We also find that CASK is SUMOylated. Conjugation of small ubiquitin-like modifier 1 (SUMO1) to CASK reduces the interaction between CASK and protein 4.1. Overexpression of a CASK–SUMO1 fusion construct, which mimicks CASK SUMOylation, impairs spine formation. Our study suggests that CASK contributes to spinogenesis and that this is controlled by SUMOylation.

Introduction

In neurons, synapse formation is initially triggered by the interaction between pre- and postsynaptic plasma membranes. Several postsynaptic transmembrane proteins, including syndecan-2 (Ethell and Yamaguchi, 1999; Lin et al., 2007), neuroligin (Nam and Chen, 2005; Varoqueaux et al., 2006), synaptic cell adhesion molecule (SynCAM; Biederer et al., 2002), and netrin G1 ligand (Kim et al., 2006), have been shown to trigger synaptogenesis. Membrane-associated guanylate kinase (MAGUK) proteins, the scaffold proteins at synapses, interact with these membrane proteins. For instance, the C-terminal tails of neuroligin and netrin G1 ligand interact with the PDZ domains of PSD-95, the prototype MAGUK protein (Irie et al., 1997; Kim et al., 2006). The C-terminal tails of syndecan-2 and SynCAM bind to the single PDZ domain of calcium/calmodulin-dependent serine protein kinase (CASK), another MAGUK protein (Hsueh et al., 1998; Biederer et al., 2002). The interactions with these synaptogenic factors suggest a potential role of PSD-95 and CASK in synapse formation. In this study, we investigate whether CASK directly regulates dendritic spinogenesis.

From the N terminus to the C terminus, the CASK protein consists of calcium/calmodulin-dependent protein kinase (CaMK)–like, L27A, L27B, PDZ, SH3, protein 4.1–binding, and guanylate kinase–like domains. All of the domains of CASK function as protein–protein interaction motifs (for review see Hsueh, 2006). Unlike PSD-95, which is highly concentrated at the postsynaptic density, CASK is widely distributed in different subcellular regions of neurons, including presynaptic buttons, postsynaptic sites, and nuclei (Hsueh and Sheng, 1999a; Hsueh et al., 1998, 2000). Via the interactions with its binding partners, CASK plays multiple roles in neurons. For instance, it forms an evolutionally conserved protein complex with Mint1/X11 and Veli/mLIN7/MALS through its N-terminal CaMK and L27 domains, respectively (Borg et al., 1998; Butz et al., 1998; Kaech et al., 1998). The interactions with Mint1 and Veli further link CASK to KIF17b and *N*-methyl-D-aspartate receptor 2b (Jo et al., 1999; Setou et al., 2000) and regulate vesicle transport of *N*-methyl-D-aspartate receptor to the synapse (Setou et al., 2000; Wong et al., 2002). This complex is involved in neurotransmitter release because knocking out Veli alters synaptic transmission (Olsen et al., 2005). CASK also interacts with liprin-α2 through the CaMK and the first L27 domains. It has

Correspondence to Yi-Ping Hsueh: yph@gate.sinica.edu.tw

Abbreviations used in this paper: CaMK, calcium/calmodulin-dependent protein kinase; CASK, calcium/calmodulin-dependent serine protein kinase; DIV, day in vitro; KS, Kolmogorov-Smirnov; MAGUK, membrane-associated guanylate kinase; MEF2, myocyte enhancer factor 2; shRNA, short hairpin RNA; SUMO, small ubiquitin-like modifier; SynCAM, synaptic cell adhesion molecule; TTX, tetrodotoxin.

The online version of this article contains supplemental material.

J. Cell Biol. Vol. 182 No. 1 141–155
www.jcb.org/cgi/doi/10.1083/jcb.200712094

been suggested that the liprin-α–CASK–Veli complex is involved in recruitment of synaptic release machinery to the presynaptic active zone (Olsen et al., 2005).

Syndecan-2, the first identified postsynaptic binding partner of the CASK PDZ domain, is a transmembrane heparan sulfate proteoglycan. It is highly concentrated at synapses (Hsueh et al., 1998), and its increased expression levels are correlated with synaptogenesis (Ethell and Yamaguchi, 1999; Hsueh and Sheng, 1999a). Knockdown of endogenous syndecan-2 inhibits spine formation in mature hippocampal neurons (Lin et al., 2007). When syndecan-2 is overexpressed in cultured hippocampal neurons at 1–2 d in vitro (DIV), it first induces filopodia formation at 4–5 DIV (Lin et al., 2007) and then promotes dendritic spinogenesis at 8–9 DIV (Ethell and Yamaguchi, 1999; Lin et al., 2007). A syndecan-2 mutant lacking the last three amino acid residues, the PDZ binding motif, loses the ability to promote spine formation but still efficiently induces filopodia formation (Lin et al., 2007). These studies suggest that the PDZ binding of syndecan-2 is important for the transformation of spines from filopodia or the maintenance of spines rather than the initiation of spinogenesis.

Because CASK also interacts with protein 4.1 (Cohen et al., 1998; Biederer and Sudhof, 2001) and because the function of protein 4.1 is to bind spectrin, a postsynaptic density protein required for synapse formation (Sytnyk et al., 2006), and to promote the interaction between spectrin and actin cytoskeleton (for reviews see Hoover and Bryant, 2000; Bretscher et al., 2002), it is reasonable to speculate that the role of CASK in spinogenesis is to link the plasma membrane proteins, such as syndecan-2 and SynCAM, to the actin cytoskeleton. In this study, we test this hypothesis using cultured hippocampal neurons. We also investigate whether the function of CASK in spinogenesis is regulated by posttranslational modification. Echoing recent exciting studies showing the role of SUMOylation in neurons (Martin et al., 2007; Shalizi et al., 2006, 2007; van Niekerk et al., 2007), we found that CASK is SUMOylated in neurons and that SUMOylation affects the interaction between CASK and protein 4.1 and alters spine morphology.

Results

CASK is required for spinogenesis

To examine the function of CASK in spine formation, RNA interference was used to knock down endogenous CASK in cultured neurons. The efficiency and specificity of a CASK short hairpin RNA (shRNA) construct were first examined in HEK and COS cells. Because the sequence of this CASK shRNA construct is identical for all human, rat, and mouse CASK genes, this shRNA was expected to knock down all human, rat, and mouse CASK genes. Compared with a nonsilencing control shRNA with no sequence homology to any mammalian gene, CASK shRNA reduced the expression of endogenous human CASK in HEK cells (Fig. 1 A) and exogenous Myc-tagged rat CASK in COS cells (Fig. 1 B). The CASK shRNA was specific for CASK because it did not affect expression of other MAGUK proteins, such as rat PSD-95 and SAP97 in COS cells (Fig. 1 B). We then examined the effect of CASK shRNA in cultured rat hippocampal neurons. At 14 DIV, cultured neurons were cotransfected with GFP-actin and either CASK shRNA or the nonsilencing control at a ratio of 3:5. Neurons were then analyzed by immunostaining at 16 DIV. CASK shRNA knocked down endogenous CASK in cultured hippocampal neurons (Fig. 1 C and Fig. S1, available at http://www.jcb.org/cgi/content/full/jcb.200712094/DC1). In general, reduction of CASK expression did not influence the global morphology of cultured hippocampal neurons (Fig. 1 C). However, in higher magnification images, compared with the nonsilencing construct, neurons transfected with CASK shRNA at 13–14 DIV had reduced spine density (Kolmogorov-Smirnov [KS] test; $D = 0.241$ and $P = 0.005$), shortened spines (KS test; $D = 0.327$ and $P < 0.001$), and narrowed spine heads (KS test; $D = 0.213$ and $P < 0.001$) at 18–19 DIV (Fig. 1, D and E). To rule out an off-target effect of CASK shRNA on spine formation, rescue experiments were performed. Overexpression of a CASK silent mutant, which was not affected by CASK shRNA (Fig. 1 B), rescued the inhibitory effect of CASK shRNA on spine density (KS test; shRNA vs. shRNA + mutant, $D = 0.221$ and $P = 0.05$; nonsilencing vs. shRNA + mutant, $D = 0.109$ and $P = 0.774$), spine length (KS test; shRNA vs. shRNA + mutant, $D = 0.299$ and $P < 0.001$; nonsilencing vs. shRNA + mutant, $D = 0.051$ and $P = 0.32$), and width of the spine head (KS test; shRNA vs. shRNA + mutant, $D = 0.17$ and $P < 0.001$; nonsilencing vs. shRNA + mutant, $D = 0.048$ and $P = 0.38$; Fig. 1, D and E), indicating a specific effect of CASK shRNA. These results suggested that reduction of CASK expression in neurons resulted in fewer and smaller dendritic spines.

We then performed time course experiments to further examine the effect of CASK shRNA on spine formation. Transfection was performed at 13 DIV, and immunostaining was performed at 15, 16, and 18 DIV (Fig. 2 A). In Fig. 1, cell morphology was outlined by GFP-actin, which is highly enriched at dendritic filopodia and spines. To rule out the role of GFP-actin in the effect of CASK shRNA, we cotransfected GFP with either CASK shRNA construct or nonsilencing control in the following experiments. Similar to the results with GFP-actin, neurons expressing GFP and CASK shRNA had fewer spines at 18 DIV (KS test; $D = 0.211$ and $P = 0.002$; Fig. 2, B and C). The length and width of spines were also shorter in CASK shRNA–expressing cells (KS test; for length, $D = 0.119$ and $P < 0.001$; for width, $D = 0.157$ and $P < 0.001$; Fig. 2, B and C). At 16 DIV, CASK shRNA–expressing cells still had fewer spines along dendrites (KS test; $D = 0.177$ and $P = 0.027$; Fig. 2, B and C). However, there were no significant differences in cumulative probability distribution between CASK shRNA and nonsilencing control in the length and width of spines (KS test; for length, $D = 0.034$ and $P = 0.344$; for width, $D = 0.017$ and $P = 0.978$; Fig. 2, B and C). At 15 DIV, although CASK protein levels had been knocked down by shRNA (Fig. S2, available at http://www.jcb.org/cgi/content/full/jcb.200712094/DC1), none of the density, length, and width parameters were affected (KS test; for density, $D = 0.075$ and $P = 0.914$; for length, $D = 0.032$ and $P = 0.614$; for width, $D = 0.040$ and $P = 0.342$; Fig. 2, B and C). These results indicate that both GFP and GFP-actin are suitable for outlining spine morphology when examining the role of CASK. They also suggest a delayed response to CASK knockdown in spine morphology.

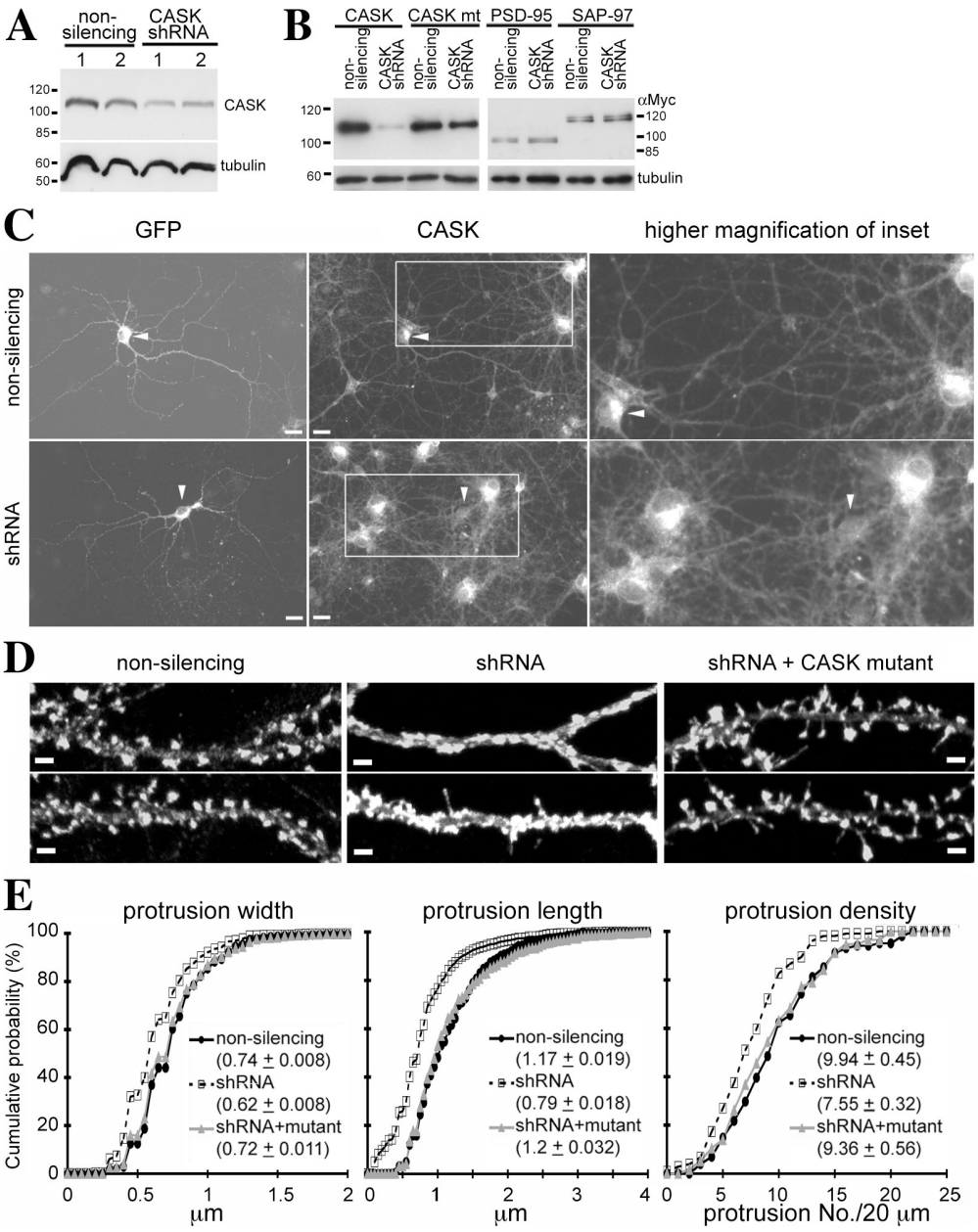

Figure 1. **Knockdown of endogenous CASK prevents dendritic spine formation in cultured hippocampal neurons.** (A) CASK shRNA reduced the expression of endogenous CASK in HEK cells. The CASK shRNA construct was transfected into HEK cells. 1 d later, cells were harvested for immunoblotting analysis using CASK and tubulin antibodies. Nonsilencing construct was used as a negative control. Tubulin was used as an internal control. (B) CASK shRNA down-regulated overexpressed Myc-tagged rat CASK but not Myc-tagged PSD-95, Myc-tagged SAP-97, or a Myc-tagged rat CASK silent mutant insensitive to CASK shRNA. COS cells were cotransfected with CASK shRNA or nonsilencing construct and various MAGUK protein expression plasmids as indicated and were harvested 1 d later for immunoblotting using Myc tag antibody. Tubulin was used as an internal control. (C) Immunostaining of cultured hippocampal neurons showing the reduction of endogenous CASK by CASK shRNA. Cultured hippocampal neurons were cotransfected with CASK shRNA construct and GFP-actin at 14 DIV. 2 d later, cells were stained with CASK antibody. Two representative images are shown. Arrowheads point to the transfected neurons, which are GFP-actin positive. Higher magnifications of the boxed areas in the middle panel are shown on the right. More images showing the knockdown effect of CASK shRNA are included in Fig. S1 (available at http://www.jcb.org/cgi/content/full/jcb.200712094/DC1). (D) CASK shRNA prevented dendritic spine formation. Cultured hippocampal neurons were cotransfected with GFP-actin and CASK shRNA, nonsilencing control, or CASK mutant resistant to CASK shRNA as indicated at 13–14 DIV. 5 d later, cells were harvested for fluorescence immunostaining using CASK (visualized by AlexaFluor594) and GFP (visualized by AlexaFluor488) antibodies. Only the GFP patterns are shown. (E) Quantification of the effect of CASK shRNA on dendritic spine morphology. For each experiment, at least 11 transfected neurons were analyzed from two independent experiments. A total of 1,027 (nonsilencing), 798 (CASK shRNA), and 549 (CASK shRNA + CASK mutant) spines were analyzed. Mean values ± SEM for each group are shown. Bars: (C) 20 μm; (D) 1 μm.

Interactions via the PDZ domain and protein 4.1–binding site are involved in CASK function in spine formation

Because several CASK PDZ domain–interacting proteins are involved in synaptic formation, we then investigated whether the role of CASK in spinogenesis is mediated by protein–protein interaction through its PDZ domain, a type II PDZ domain. Two dominant-negative mutants that interrupt the interactions between endogenous CASK and the PDZ-binding molecules, the CASK PDZ domain alone (PDZ) and the cytoplasmic tail

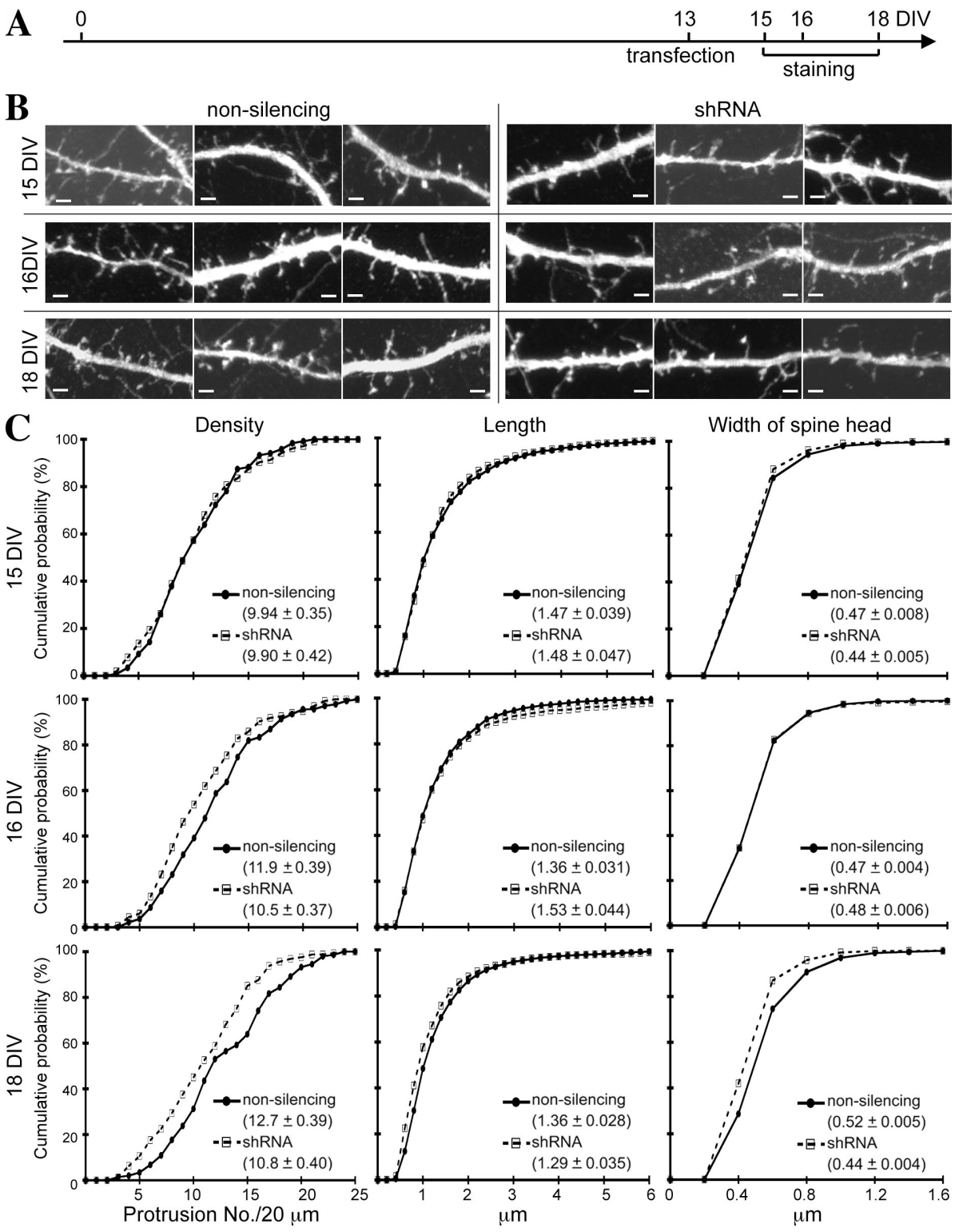

Figure 2. **Time course of CASK knockdown changes in spine morphology.** (A) CASK shRNA and nonsilencing control were cotransfected with GFP into hippocampal neurons at 13 DIV. Immunostaining using CASK and GFP antibodies were performed at 15, 16, and 18 DIV as indicated. (B) Representative images of neurons transfected with CASK shRNA and nonsilencing control. Only the GFP signals are shown to outline the morphology of dendrites. The effect of CASK shRNA on down-regulation of CASK protein levels is shown in Fig. S2 (available at http://www.jcb.org/cgi/content/full/jcb.200712094/DC1). (C) Quantification analysis. More than 14 neurons collected from two independent experiments were analyzed for each group. The total number of spines analyzed in each group was as follows: 15 DIV, 1,225 nonsilencing and 1,028 CASK shRNA; 16 DIV, 1,660 nonsilencing and 1,420 CASK shRNA; and 18 DIV, 1,878 nonsilencing and 1,730 CASK shRNA. Mean values ± SEM for each group are shown. Bars, 2 μm.

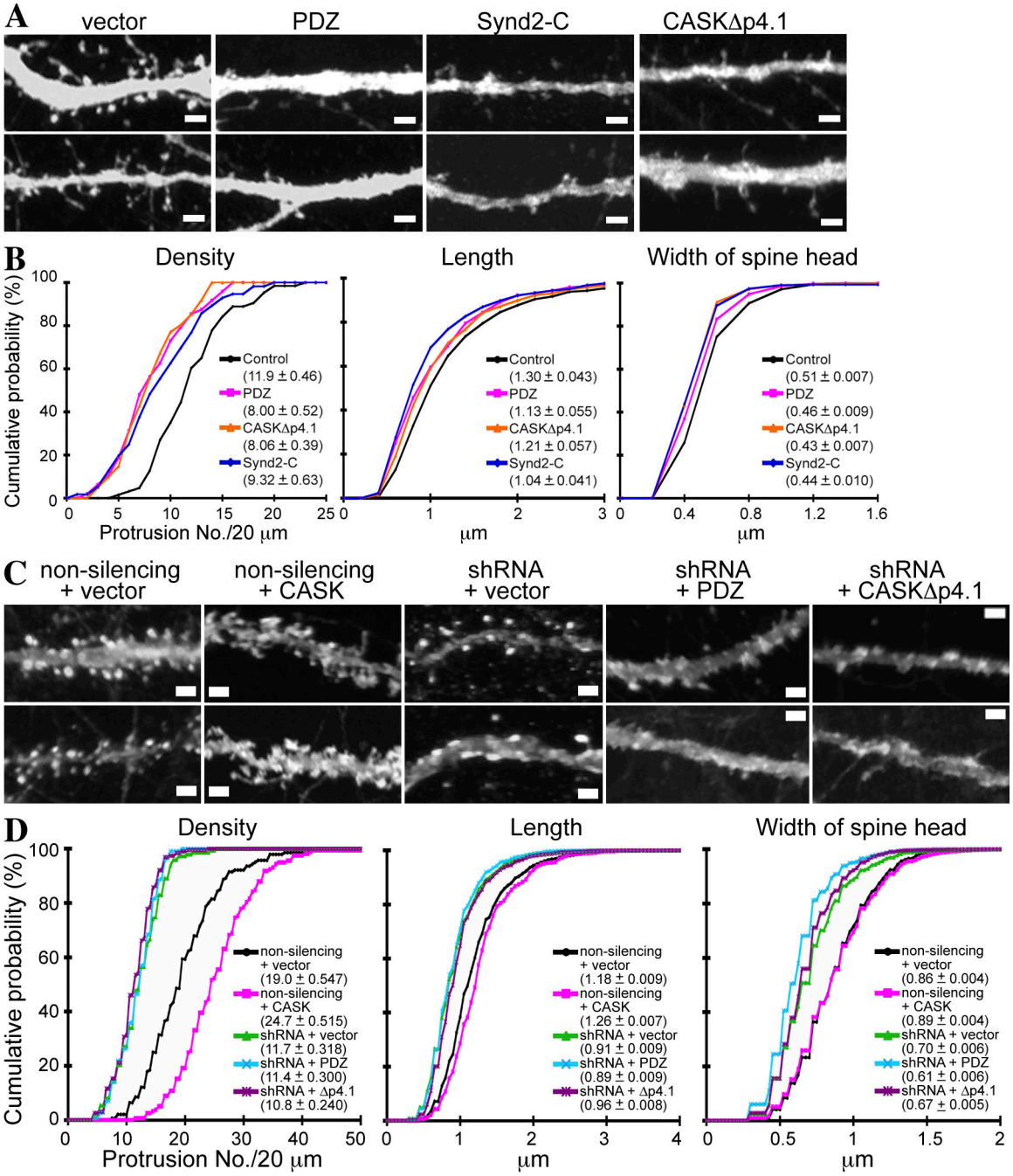

Figure 3. **The PDZ domain and protein 4.1–binding site of CASK are involved in dendritic spine formation.** (A) Overexpression of CASK PDZ domain (PDZ), the C-terminal tail of syndecan-2 (synd-2C), and the CASKΔp4.1 mutant prevented spinogenesis. Cultured hippocampal neurons were cotransfected with GFP and various constructs as indicated at 13 DIV. 5 d later, cells were harvested for immunostaining using HA tag and GFP antibodies. Only the GFP patterns are shown. (B) Quantitative analysis of A. The total number of spines analyzed in each group was 756 GW1 control, 385 PDZ, 535 Synd-2C, and 494 CASKΔp4.1. More than 10 neurons for each group were analyzed. Mean ± SEM for each group is shown. (C) Overexpression of the CASK PDZ domain and CASKΔp4.1 mutant does not rescue the phenotype of CASK knockdown. At 12 DIV, cultured hippocampal neurons were cotransfected with GFP-actin and various constructs as indicated. Immunostaining using CASK, HA tag, and GFP antibodies was performed at 18 DIV. Only GFP patterns are shown. (D) Quantitative analysis of C. The total number of neurons and spines analyzed in each group was as follows: nonsilencing + GW1 vector, 31 and 2,703; nonsilencing + CASK, 27 and 4,037; shRNA + GW1 vector, 31 and 1,754; shRNA + PDZ, 32 and 1,317; and shRNA + Δp4.1, 31 and 2,085. Mean ± SEM for each group is shown. Bars, 2 μm.

of syndecan-2 (synd-2C), were cotransfected with GFP into cultured hippocampal neurons. Similar to the results using CASK shRNA, overexpression of the CASK PDZ domain also resulted in fewer, shorter, and smaller spines compared with vector control (KS test; for density, $D = 0.456$ and $P < 0.001$; for length, $D = 0.135$ and $P = 0.011$; for width, $D = 0.115$ and $P = 0.047$; Fig. 3, A and B). When the construct expressing the C-terminal tail of syndecan-2 was introduced into neurons, the density, length, and width of spines were also reduced (KS test; for density, $D = 0.373$ and $P < 0.001$; for length, $D = 0.206$ and $P < 0.001$; for width, $D = 0.230$ and $P < 0.001$; Fig. 3, A and B).

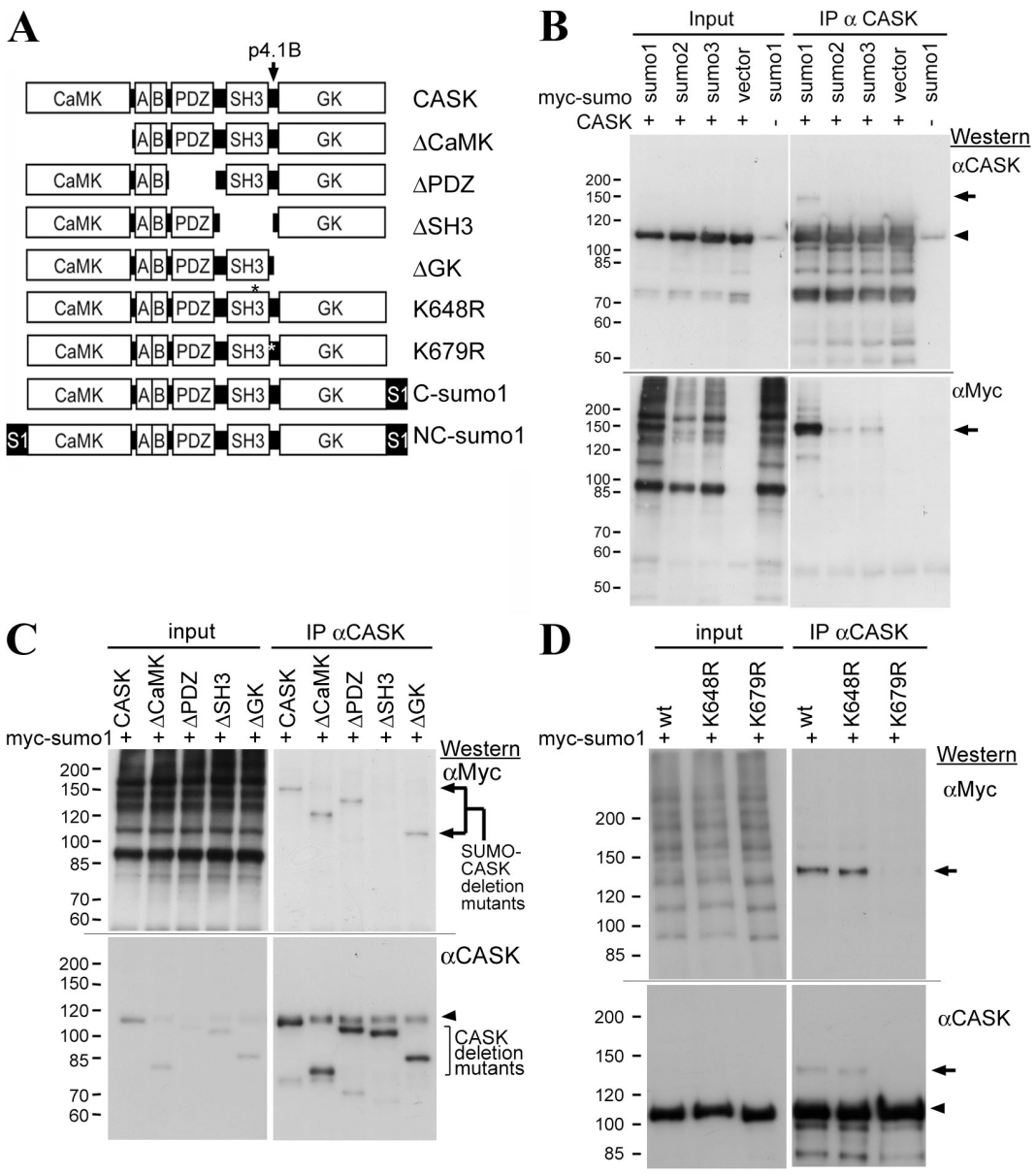

Figure 4. **CASK is modified by SUMO1 at residue K679.** (A) A schematic diagram of CASK, CASK deletion mutants, and SUMO1-CASK fusions. Some of the constructs had two versions: one was Myc tagged at the N-terminal end, and the other had no extra tag. (B) COS1 cells were cotransfected with plasmids expressing 1 μg Myc-tagged SUMO1, 2, or 3 and 1 μg CASK. After 24-h incubation, total cell extracts were harvested and immunoprecipitated with CASK antibody. Immunoblotting analysis was then performed sequentially using CASK antibody to monitor CASK proteins and Myc tag antibody to detect Myc-tagged SUMOs. (C) 1.2 μg CASK deletion mutants was cotransfected with 0.4 μg SUMO1 into COS1 cells to evaluate the SUMO1-modified region of CASK by immunoprecipitation-immunoblotting analysis as described in B except that Myc tag antibody was used first for immunoblotting. The arrowhead points to the position of endogenous full-length CASK in COS1 cells. Arrows indicate the positions of SUMO1-CASK deletion mutants. (D) Two putative SUMO1-modified consensus motifs, guanylate kinase^{648}LE and TK^{679}QE, were predicted in the sequence of rat CASK, and site-directed mutagenesis was performed to change lysine 648 and 679 to arginine. COS1 cells were cotransfected with 0.5 μg SUMO1 and 0.5 μg of wild-type CASK, K648R, or K679R mutant and subjected to immunoprecipitation-immunoblotting analysis. (B and D) Arrows indicate the positions of SUMOylated CASK; arrowheads point to the positions of unmodified full-length CASK.

We then wondered whether the CASK protein 4.1–binding site is also required for spinogenesis. Because the protein 4.1–binding site covers only around 10 amino acid residues, it was inconvenient to simply express the protein 4.1–binding site alone to interrupt the interaction between endogenous CASK and protein 4.1. Instead, a CASK mutant lacking the protein 4.1–binding motif was introduced into cultured hippocampal neurons (Fig. 3 A), and quantitative analyses showed that compared with GFP alone, overexpression of this CASKΔp4.1 mutant also reduced the density and length of spines and the width of spine heads (KS test; for density, $D = 0.447$ and $P < 0.001$; for length, $D = 0.114$ and $P = 0.025$; for width, $D = 0.231$ and $P < 0.001$; Fig. 3, A and B).

The effect of these CASK mutants in spine morphology was also examined in the presence of CASK shRNA. Similar to the results in Fig. 1, the morphology and density of dendritic spines were impaired by reducing the protein levels of endogenous CASK (nonsilencing + vector GW1 vs. CASK shRNA +

vector GW1; for density, D = 0.539 and P < 0.001; for length, D = 0.317 and P < 0.001; for width, D = 0.283 and P < 0.001; Fig. 3, C and D). Overexpression of the CASK PDZ domain or CASKΔp4.1 mutant did not rescue the spine phenotype seen in CASK knockdown (Fig. 3, C and D). These results suggested that the PDZ domain and protein 4.1–binding sites of CASK have to be present in the same molecule to perform their functions in spine morphology. When CASK was overexpressed, the spine density was increased (nonsilencing control + vector control vs. nonsilencing control + CASK; D = 0.406 and P < 0.001; Fig. 3, C and D). However, CASK overexpression did not appear to further enlarge spine heads (Fig. 3, C and D). Collectively with the result in Fig. 2, it suggests that CASK functions as a molecule stabilizing or maintaining spine morphology rather than a factor triggering spine enlargement.

CASK proteins are SUMOylated

We then wonder whether the activity of CASK in spinogenesis is regulated by posttranslational modification. According to sequence analysis using the program SUMOPlot (Abgent), several putative SUMOylation sites on CASK protein were predicted, including K20, K60, K70, K159, K192, K615, K648, K716, K762, and K763. Among these sites, K648 and K716 are very close to the protein 4.1–binding site (residues 685–697 of rat CASK; Fig. 4 A). Because SUMOylation usually modifies target protein–protein interaction, distribution, or activity, we wondered whether CASK is SUMOylated and whether CASK SUMOylation affects the interaction between CASK and protein 4.1 and thus regulates the function of CASK in spinogenesis. In mammals, four small ubiquitin-like modifiers (SUMOs) have been identified, SUMO1–4. Among them, SUMO4 is the least studied. Whether SUMO1, SUMO2, or SUMO3 are conjugated to CASK proteins was investigated by cotransfecting CASK and Myc-tagged SUMOs into COS cells followed by immunoprecipitation using CASK antibody. In addition to 110-kD full-length CASK protein, an extra protein species at ∼140–150 kD was also revealed by CASK antibody from cells transfected with Myc-SUMO1 (Fig. 4 B, top; arrow). To confirm that this extra protein band represented SUMOylated CASK, the membrane was stripped and reprobed with Myc tag antibody. A prominent Myc tag immunoreactivity was present in the product precipitated by CASK antibody from cells cotransfected with CASK and Myc-SUMO1 (Fig. 4 B, bottom; arrow). These data support SUMO modification of CASK in COS cells. Although SUMO2 and SUMO3 could also be conjugated with CASK, the efficiency was much lower than for SUMO1. Therefore, we focused on SUMO1 in the following experiments.

To identify the SUMOylation site of CASK, a series of CASK domain deletion mutants (Fig. 4 A) were cotransfected with Myc-tagged SUMO1 into COS cells. Immunoprecipitation/immunoblotting analysis was then performed to examine SUMOylation of these deletion mutants. The deletion of SH3 domain by removing amino acid residues 598–682 of rat CASK impaired CASK SUMOylation (Fig. 4 C). From the computational prediction, K648 is the only SUMOylation site within this region. However, a K648R mutation was not able to abolish the SUMOylation (Fig. 4 D). We then looked closer at the sequence in this region and predicted residue K679 to be a potential SUMOylation site. Indeed, a K679R mutation inhibited CASK SUMOylation (Fig. 4 D) and indicated that residue K679 is the SUMOylation site of rat CASK protein.

CASK SUMOylation reduces the interaction between CASK and protein 4.1

Because SUMOylation has been suggested to regulate nuclear translocation (for reviews see Wilson and Rangasamy, 2001; Pichler and Melchior, 2002) and because CASK is able to enter the nucleus and regulate gene expression (Hsueh et al., 2000), we examined whether SUMOylation of CASK promotes the nuclear translocation of CASK. In addition to the CASK K679R mutant, which impairs the SUMOylation of CASK, SUMO1 was fused with CASK at either the C-terminal or both N- and C-terminal ends of CASK to mimic SUMOylated CASK (Fig. 4 A). These constructs were expressed in COS cells. Nuclear distribution of CASK was then examined by immunofluorescence staining and confocal analysis. Similar to wild-type CASK, the majority of K679R, C-SUMO1-CASK, and NC-SUMO1-CASK mutants were still present in the cytoplasm of transfected COS cells (Fig. 5 A), indicating that SUMOylation does not trigger the nuclear translocation of CASK.

We then wondered whether CASK SUMOylation regulates the interaction between CASK and protein 4.1. Two experiments were performed to address this possibility. First, the Myc-tagged wild-type CASK, K679R mutant, C-SUMO1-CASK, and NC-SUMO1-CASK constructs were cotransfected with FLAG-tagged protein 4.1N into COS cells. Coimmunoprecipitation was performed using FLAG antibody. Compared with wild-type CASK, FLAG antibody precipitated less C-SUMO1-CASK and NC-SUMO1-CASK (Fig. 5 B), indicating that the interaction between protein 4.1N and C-SUMO1-CASK or NC-SUMO1-CASK was lower than with wild-type CASK.

The second experiment overexpressed SUMO1 with CASK and protein 4.1N and investigated whether SUMO1 overexpression impaired the interaction between CASK and protein 4.1N. Although <10% of CASK protein was SUMOylated in COS cells (Figs. 4 B and 5 C, input lanes), SUMO1 overexpression resulted in a 60% reduction of the interaction between CASK and protein 4.1N (Fig. 5 C). Perhaps CASK SUMOylation in COS cells was underestimated because deSUMOylation may occur immediately after SUMOylated proteins performed their functions in cells and because isopeptidase activity is extremely high after cell lysis. No matter which explanation is the correct one, these results support the idea that SUMOylation of CASK regulates the protein–protein interaction between CASK and protein 4.1.

Because protein 4.1 interacts with spectrin and promotes the interaction between spectrin and filamentous actin, reduction of the interaction between CASK and protein 4.1 by SUMOylation would be expected to attenuate the association between CASK and filamentous actin. To test this possibility, protein 4.1N was cotransfected with wild-type CASK, C-SUMO1-CASK, or NC-SUMO1-CASK into COS cells. Coimmunoprecipitation was then performed using actin antibodies. Consistent with the results of coimmunoprecipitation with protein 4.1N,

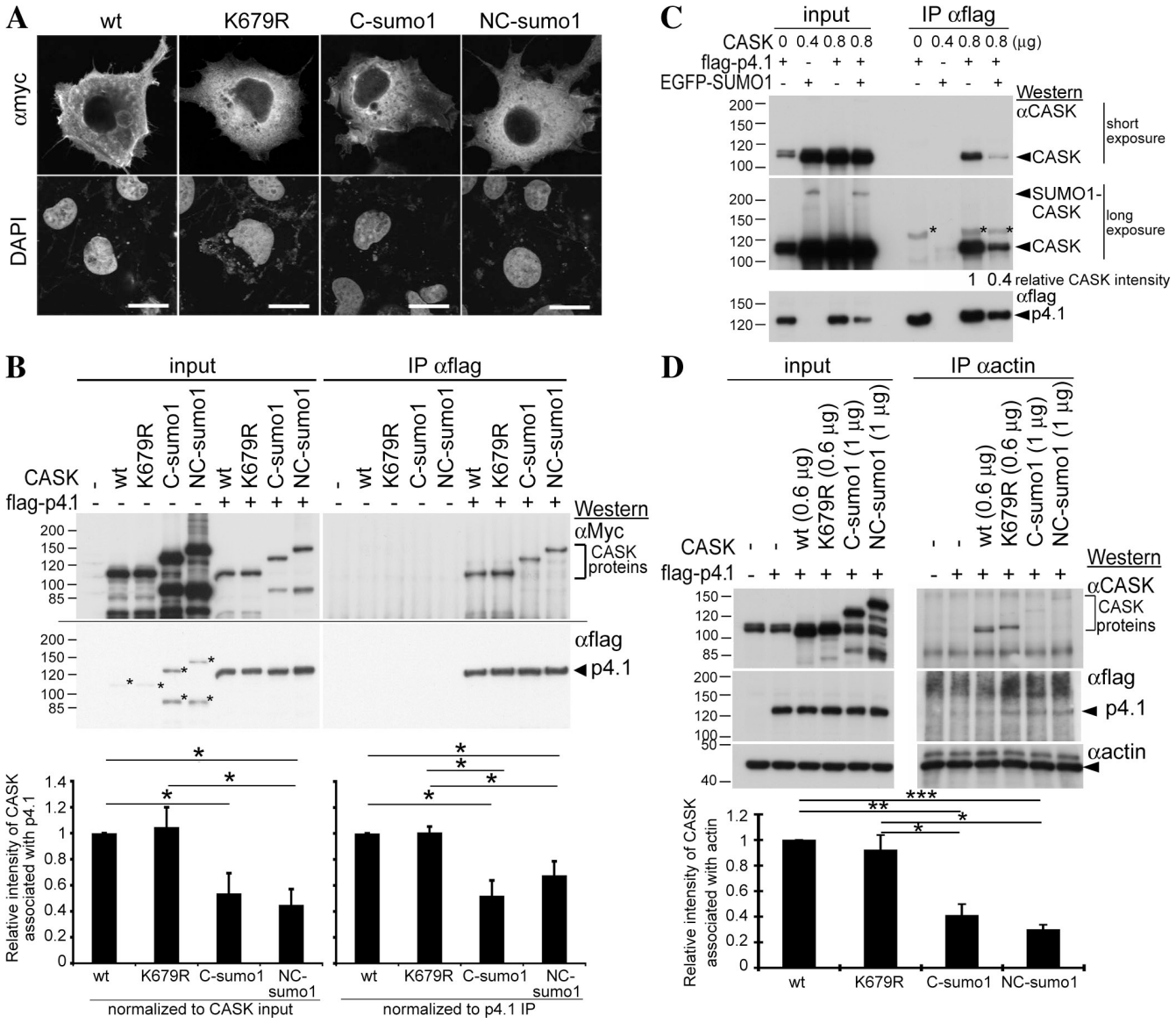

Figure 5. **SUMOylation does not promote nuclear distribution of CASK but interferes with the interaction between CASK and protein 4.1N in COS cells.** (A) Confocal analysis of the subcellular distribution of CASK proteins. Myc-tagged wild-type and CASK mutants were transfected into COS1 cells as indicated. Nuclei were counterstained with DAPI. (B) The interaction between protein 4.1N and CASK. COS1 cells were cotransfected with 0.25 μg FLAG-tagged protein 4.1N and either 1 μg Myc-tagged CASK or 1 μg CASK mutants as indicated. Immunoprecipitation was performed using FLAG tag antibody. The precipitates were analyzed by immunoblotting using specific antibodies to the Myc and FLAG tags sequentially. The asterisks indicate the residual Myc immunoreactivities from the top panel. The protein levels of coimmunoprecipitated CASK were analyzed by ImageJ version 1.38X (National Institutes of Health). The data presented are the mean ± SEM of three independent experiments. The relative amounts of proteins were normalized to the amounts of CASK input and precipitated protein 4.1 as indicated. The significance of any difference was determined by *t* test using SPSS software, and significant differences are shown; *, $P < 0.05$. (C) Overexpression of SUMO1 reduces the interaction between CASK and protein 4.1N. COS cells were triple transfected with CASK, flag-tagged protein 4.1N, and GFP-tagged SUMO1 or vector control and analyzed by immunoprecipitation-immunoblotting using antibodies as indicated. The DNA amounts for transfection are also shown. Because cotransfection with protein 4.1N reduces CASK amounts in the Triton X-100–solubilized lysate (see B), the DNA amounts for transfection were adjusted accordingly to make the CASK protein amounts similar among different groups. The relative protein amounts of CASK coimmunoprecipitated with protein 4.1N were normalized to both precipitated protein 4.1N amounts and CASK input amount. The data are means of two independent experiments. The asterisks indicate the nonspecific signals contributed by precipitated protein 4.1N. (D) SUMOylation reduces the association of CASK with actin cytoskeleton. COS cells were cotransfected with protein 4.1N and CASK constructs as indicated. Immunoprecipitation was performed using actin antibody and analyzed by immunoblotting using antibodies as indicated. The amount of CASK protein coimmunoprecipitated with actin, normalized to actin precipitated amounts, is shown. Data are the means of three independent experiments. Error bars indicate SEM. *, $P < 0.05$; **, $P < 0.005$; ***, $P < 0.001$. Bars, 20 μm.

the interaction between actin and C-SUMO1-CASK or NC-SUMO1-CASK was greatly reduced compared with wild-type CASK or K679R mutant (Fig. 5 D), supporting the idea that the association of CASK with actin cytoskeleton is regulated by CASK SUMOylation.

SUMOylated CASK proteins are present at synapses

To investigate whether CASK is SUMOylated in the brain, rat brain extracts purified from cerebral cortex and midbrain were immunoprecipitated by CASK antibody and analyzed by

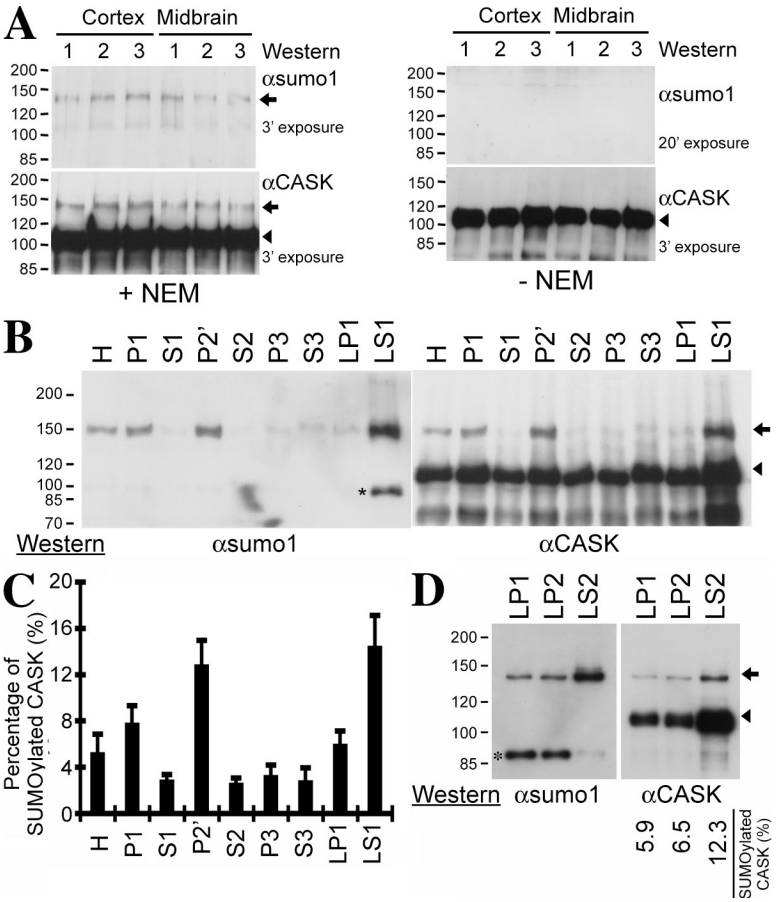

Figure 6. **SUMOylated CASK proteins are present in the mouse brain.** (A) Mouse brain homogenates purified from three different mice in the presence or absence of *N*-ethylmaleimide were immunoprecipitated with CASK antibody. The precipitates were then analyzed by immunoblotting using SUMO1 and CASK antibodies sequentially. The exposure time for each image is indicated. (B) Mouse brain subcellular fractions prepared as described in Materials and methods were used to examine the neuronal distribution of SUMOylated CASK. Equal amounts of each fraction were analyzed by immunoprecipitation-immunoblotting analysis as described in A. H, total homogenate; P1, nuclei and cell debris; S1, supernatant of P1; P2′, washed crude synaptosomal fraction; S2, supernatant of P2′; LP1, lysed synaptosomal membrane; LS1, supernatant of LP1; P3, light membrane fraction; S3, soluble cytosol. The asterisk indicates an unknown protein species recognized by SUMO1 antibody. (C) The percentage of SUMOylated CASK in total CASK proteins of each subcellular fraction. The protein levels of SUMOylated CASK and nonSUMOylated CASK were analyzed using ImageJ. For each fraction, the percentage of SUMOylated CASK was determined by dividing the amounts of SUMOylated CASK by the sum of SUMOylated and nonSUMOylated CASK. The data presented are the mean ± SEM (error bars) of four independent experiments. (D) SUMOylated CASK is mostly present in synaptic cytosol, LS2 fraction. The LS1 fraction was further separated into LP2 fraction, crude synaptic vesicles, and LS2 fraction, synaptic cytosol. CASK proteins were immunoprecipitated from equal protein amounts of LP1, LP2, and LS2 fractions and analyzed by immunoblotting using SUMO1 and CASK antibodies as indicated. The percentage of SUMOylated CASK in total CASK proteins is also indicated. (A, B, and D) Arrows indicate the positions of SUMOylated CASK; arrowheads point to the positions of unmodified full-length CASK.

immunoblotting using SUMO1 and CASK antibodies sequentially. SUMO1 antibody detected a protein species at around 140–150 kD in the precipitates from cerebral cortex as well as from midbrain (Fig. 6 A, top left; +NEM). This protein species was also revealed by immunoblotting using CASK antibody (Fig. 6 A, bottom left; +NEM). In extracts that did not include *N*-ethylmaleimide to prevent deSUMOylation, the protein species at 140–150 kD could not be detected by either SUMO1 or CASK antibody (Fig. 6 A, right; −NEM), confirming that the protein species at around 140–150 kD is SUMOylated CASK.

We then examined where SUMOylated CASK is present in neurons. A series of centrifugation steps were performed to isolate washed crude synaptosomal membrane (P2′), light membrane (P3), soluble cytosolic (S3), and lysed synaptosomal membrane fractions (LP1) as well as a fraction containing synaptic cytosol and crude synaptic vesicles (LS1). Equal protein amounts of these fractions were then subjected to immunoprecipitation using CASK antibody followed by immunoblotting using SUMO1 and CASK antibodies sequentially. SUMOylated CASK protein was highly concentrated in the LS1 fraction, although trace amounts of SUMOylated CASK protein were also detectable in the LP1, P3, and S3 fractions (Fig. 6, B and C). We then further separated the LS1 fraction into LP2 (crude synaptic vesicles) and LS2 (synaptic cytosol) fractions and checked the distribution of SUMOylated CASK in these two fractions. In the LS2 fraction, ∼12% of CASK was SUMOylated. In contrast, ∼6% of CASK protein was SUMOylated in the LP2 fraction (Fig. 6 D). These data indicate that SUMOylated CASK proteins are mainly associated with the synaptic cytosol. SUMOylation may promote the dissociation of CASK from the membrane.

Indirect immunofluorescence staining using SUMO1, CASK, and PSD-95 antibodies was also performed to confirm synaptic distribution of SUMOylated CASK. Under normal culture conditions, SUMO1 antibody did not give any obvious signal along the dendrites (Fig. 7 A, control panel). Because kainate treatment has been shown to specifically induce SUMOylation of kainate receptors (Martin et al., 2007), we wondered whether general neuronal activity regulates protein SUMOylation at synapses. To address this issue, neurons were treated with tetrodotoxin (TTX) overnight to reduce their activity. After washing out TTX, neurons were immediately incubated in 60 mM potassium chloride for 3 min. 20–40 min later, neurons were immunofluorescence stained. After depolarization, SUMO1 immunoreactivity became stronger and very punctate along dendrites compared with neurons treated with either TTX alone or no treatment (Fig. 7 A). After depolarization in high KCl solution, the number of SUMO1 puncta was more than double that of the TTX-treated and control neurons (Fig. 7 B). More than 85% of SUMO1 puncta were colocalized with postsynaptic marker PSD-95 (Fig. 7 C), indicating a synaptic distribution of SUMO1 conjugates after depolarization. Among these synaptic SUMO1 puncta, ∼50% of them were CASK positive (Fig. 7, B and C), which is consistent with the results of biochemical fractionation that suggested that SUMOylated CASK proteins were concentrated in the synaptic cytoplasm (Fig. 6).

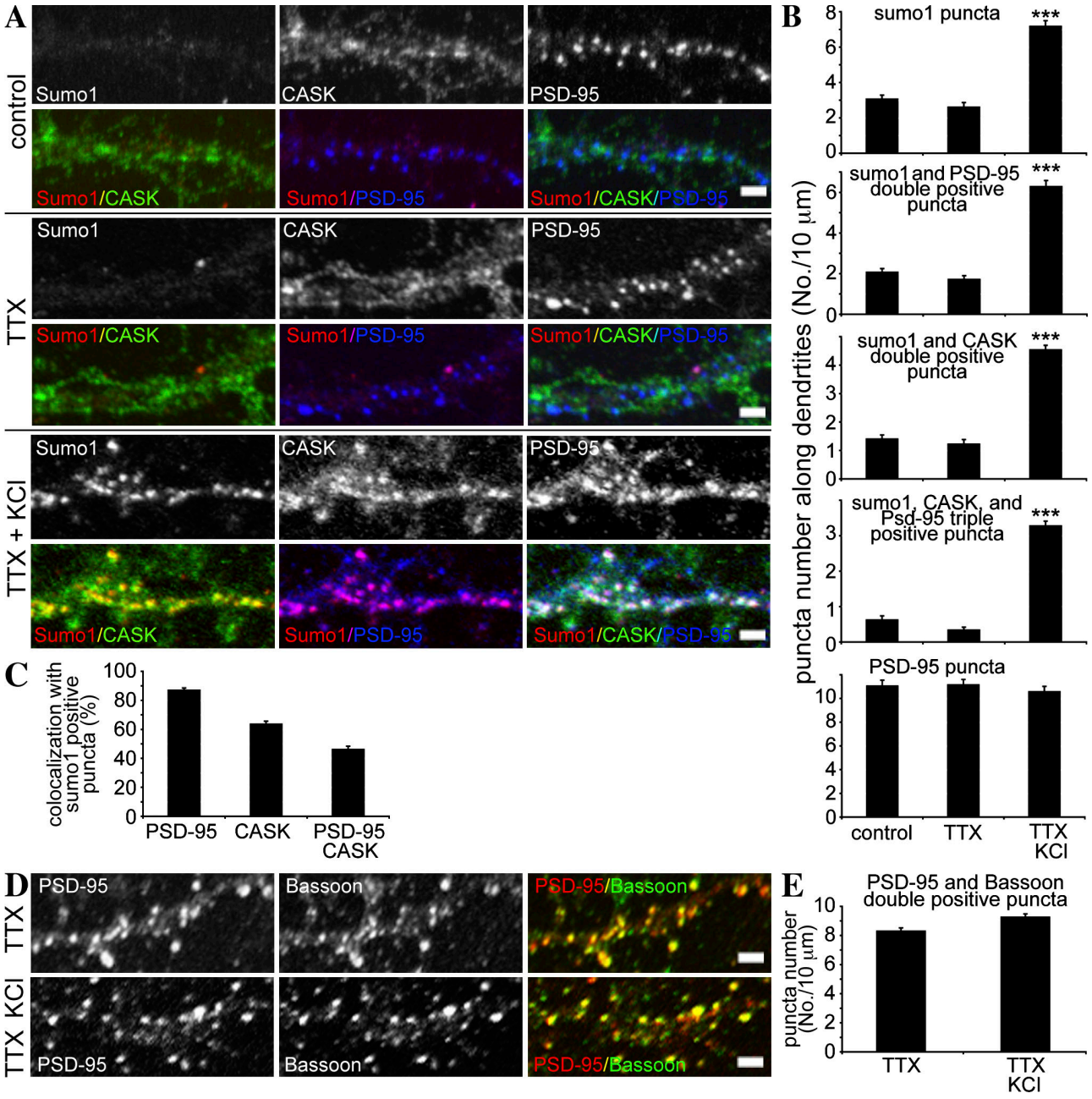

Figure 7. **Synaptic distribution of SUMOylated CASK.** (A) At 16–17 DIV, cultured hippocampal neurons were divided into three different groups: (1) untreated control, (2) 1 μM TTX overnight, and (3) overnight TTX followed by 60 mM KCl for 3 min. 20–40 min after removing KCl, cells were fixed and stained with SUMO1, CASK, and PSD-95 antibodies. (B) Quantification of SUMO1, CASK, and PSD-95 puncta along dendrites. More than 80 dendrites from >22 neurons were analyzed for each group. Mean values ± SEM (error bars) are shown. ***, $P < 0.001$ by *t* test. (C) The percentage of PSD-95, CASK, and PSD-95–CASK double-positive puncta in the population of SUMO1-positive puncta along dendrites. (D) Colocalization of PSD-95 and Bassoon along dendrites of neurons treated with TTX alone and TTX followed by potassium chloride. (E) Quantification analysis of PSD-95 and Bassoon double-positive puncta. More than 80 dendrites from >18 neurons were analyzed in each group. Mean values ± SEM are shown. Bars, 2 μm.

To confirm that the postsynaptic distribution of PSD-95 is not altered by depolarization, we first counted the number of PSD-95 puncta along dendrites; this was not significantly different between neurons treated with TTX and high potassium, TTX alone, or in the control (Fig. 7 B). Double immunofluorescence staining using PSD-95 and the presynaptic marker Bassoon was then performed to examine pre- and postsynaptic connections after depolarization. The densities of PSD-95 and Bassoon double-positive puncta were comparable between TTX-treated neurons and depolarized neurons (Fig. 7, D and E), suggesting that the synaptic distribution of PSD-95 did not change upon synaptic stimulation.

SUMOylation of CASK influences spine morphogenesis

Because SUMOylation of CASK regulates the interaction between CASK and protein 4.1 and because the interaction with protein 4.1 is required for CASK function in spinogenesis, we then

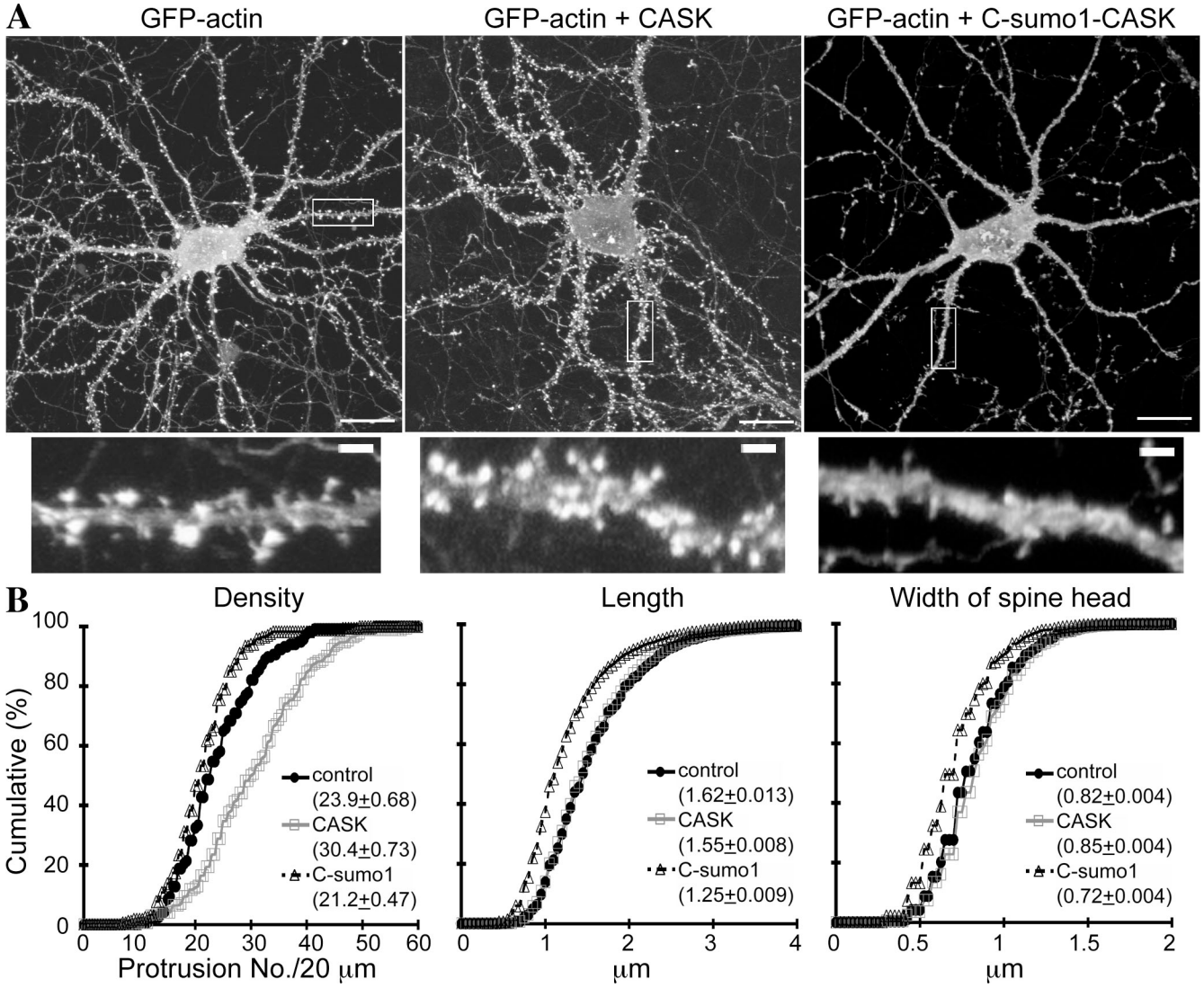

Figure 8. **SUMOylation of CASK influences dendritic spine morphology.** (A) Hippocampal neurons were cotransfected with GFP-actin and Myc-CASK, Myc-C-SUMO1-CASK, or vector control at a ratio of 1:5 at 10–12 DIV as indicated and were fixed at 17–18 DIV to examine spine morphology by double staining using Myc and GFP antibodies. Only double-positive neurons were collected for analysis. The images of GFP signal are shown. Myc tag signal revealing the patterns of CASK and C-SUMO1-CASK are shown in Fig. S3 (available at http://www.jcb.org/cgi/content/full/jcb.200712094/DC1). The bottom panel shows higher magnification of the boxed areas in the top panel. (B) Quantification of spine density, length, and width from A. The histograms show the cumulative distribution as a percentage. A total of 2,828 (GFP-actin alone), 5,229 (Myc-CASK), and 3,586 (Myc-C-SUMO1-CASK) spines from >117 dendrites of >22 neurons were analyzed. Mean values ± SEM for each group are shown in the insets. Bars: (A, top) 20 μm; (A, bottom) 2 μm.

investigated whether CASK SUMOylation modulates spine formation. GFP-actin was cotransfected with Myc-tagged wild-type CASK, Myc-tagged C-SUMO1-CASK, or vector control into cultured hippocampal neurons at 10 DIV. Cells were then fixed at 17–18 DIV for immunofluorescence staining. Compared with wild-type CASK or vector control, the expression of C-SUMO1-CASK significantly narrowed the width (GFP-actin + C-SUMO1-CASK vs. GFP-actin, $D = 0.261$ and $P < 0.001$; GFP-actin + C-SUMO1-CASK vs. GFP-actin + CASK, $D = 0.275$ and $P < 0.001$; Fig. 8;), shortened the length (GFP-actin + C-SUMO1-CASK vs. GFP-actin, $D = 0.299$ and $P < 0.001$; GFP-actin + C-SUMO1-CASK vs. GFP-actin + CASK, $D = 0.273$ and $P < 0.001$; Fig. 8), and reduced the density of spines (GFP-actin + C-SUMO1-CASK vs. GFP-actin, $D = 0.190$ and $P = 0.0143$; GFP-actin + C-SUMO1-CASK vs. GFP-actin + CASK, $D = 0.486$ and $P < 0.001$; Fig. 8). Similar to the results in Fig. 3 (C and D), overexpression of CASK significantly increased the spine density compared with vector control ($D = 0.334$ and $P < 0.001$; Fig. 8). These results suggest that the SUMOylation of CASK impairs spine formation.

The distribution of C-SUMO1-CASK in neurons was also examined. Similar to the wild-type CASK, C-SUMO1-CASK was widely distributed in cultured hippocampal neurons, including in the soma, dendrites, and axons (Fig. S3, available at http://www.jcb.org/cgi/content/full/jcb.200712094/DC1). Along dendrites, in addition to a diffuse distribution in the dendritic shaft, wild-type CASK also displayed a punctate pattern colocalized with GFP-actin at spines. Less punctate signal was observed for C-SUMO1-CASK (Fig. S3), which may be caused by either impairment of spine formation by C-SUMO1-CASK or an attenuation of the interaction between C-SUMO1-CASK and protein 4.1.

Discussion

In this study, we used RNA interference and dominant-negative mutant approaches to demonstrate the role of CASK in dendritic spinogenesis. We also identified SUMOylation as a posttranslational modification of CASK that regulates the interaction between CASK and protein 4.1 and, thus, modulates spinogenesis. In addition to spinogenesis, CASK also acts presynaptically to regulate synaptogenesis through a different mechanism: CDK5 phosphorylates residues S51 and S395 of CASK proteins, which enhances the interaction between CASK and N-type calcium channels but impairs the interaction between CASK and liprin-α (Samuels et al., 2007). Because CASK is involved in synaptic targeting of N-type calcium channels (Maximov and Bezprozvanny, 2002), phosphorylation of CASK by CDK5 modulates presynaptic calcium influx and controls synapse formation (Samuels et al., 2007). Collectively, through different binding partners and different posttranslational modifications, CASK regulates synaptogenesis in both pre- and postsynaptic ways.

Recently, CASK knockout mice have been produced (Atasoy et al., 2007). Consistent with the phenotype of mice carrying an insertional mutation in the CASK gene (Laverty and Wilson, 1998), deletion of the CASK gene results in lethality within 1 d after birth. Although glutamatergic miniature excitatory postsynaptic potential frequency is increased and GABAergic miniature excitatory postsynaptic potential frequency is decreased, cultured cortical neurons isolated from CASK-deficient mice form synapses at a similar density to wild-type neurons at 14 DIV (Atasoy et al., 2007). This is not the only case in which the results of a mouse knockout conflict with those of RNA interference knockdown. Gene target mutation of PSD-95 fails to alter glutamatergic synaptic transmission (Migaud et al., 1998). However, knockdown of PSD-95 in cultured hippocampal neurons reduces synaptic targeting of glutamate receptor 2 and the event frequency of AMPAR excitatory postsynaptic currents (Elias et al., 2006). Compensation of the phenotype of PSD-95 knockout mice by other MAGUK proteins, such as PSD-93, has been proposed (Elias et al., 2006). For CASK, it is also possible that molecular redundancy among CASK and other MAGUK proteins (for review see Hsueh, 2006) play a role in modulating the spinogenesis phenotype of CASK knockout mice. Another possibility is the result of selection in vitro during culture. Atasoy et al. (2007) found more apoptotic cells in the CASK-deficient brain, suggesting a role of CASK in neuronal survival. In the cerebral cortex, some neurons express higher levels of CASK, whereas other neurons express very low levels of CASK (Hsueh et al., 1998). When cortical neurons are cultured in vitro for 14 d, this may select neurons that originally have a very low level of CASK. The difference in spinogenesis between CASK-deficient neurons and wild-type neurons therefore cannot be found after 14 d in culture. In our experiment, CASK was knocked down at 13–14 DIV; the effect of CASK on spinogenesis was then monitored at 18–19 DIV. This can avoid the secondary effect of long-term selection during culture.

In our previous study, we found that two cytoplasmic motifs of syndecan-2 are involved in two sequential processes of spinogenesis: the C1 region of syndecan-2 interacts with neurofibromin and promotes filopodia formation; the C2 region then transforms filopodia to dendritic spines (Lin et al., 2007). The results indicated that the C2-binding proteins contribute to the transformation of dendritic spines from filopodia. Several C2-binding proteins have been identified, including CASK, syntenin, synbindin, and synectin (Grootjans et al., 1997; Cohen et al., 1998; Hsueh et al., 1998; Ethell et al., 2000; Gao et al., 2000). Although we have not tested other C2-binding proteins, in this study, we show that CASK contributes to dendritic spinogenesis. Our results suggest that both the PDZ domain and the protein 4.1–binding motif are involved in spine formation. Because protein 4.1 binds spectrin, an abundant component at the postsynaptic density, and thus promotes the interaction between spectrin and filamentous actin (for reviews see Hoover and Bryant, 2000; Bretscher et al., 2002), CASK may act as a linker between transmembrane proteins and the actin cytoskeleton and, therefore, stabilize dendritic spines. Because CASK and protein 4.1 are widely expressed in different tissues, SUMOylation of CASK may also regulate the interaction between CASK and protein 4.1 in nonneuronal cells. CASK-deficient mice show a cleft palate phenotype (Laverty and Wilson, 1998; Atasoy et al., 2007). Consistent with this phenotype, SUMO1 haploinsufficiency has been shown to result in cleft palate (Alkuraya et al., 2006). In addition to spinogenesis, it is likely that the SUMOylation of CASK also contributes to craniofacial development.

Our results also suggest that CASK tends to modulate spinogenesis late. At 15 DIV, 2 d after the expression of CASK shRNA, CASK protein levels were knocked down (Fig. S2). Longer incubation times, such as 3 or 5 d after transfection of CASK shRNA, did not appear to further reduce the CASK protein levels (Fig. S2). However, the spine morphology of CASK knockdown neurons was comparable with neurons transfected with vector control at 15 DIV (Fig. 2 B). One extra day later (16 DIV), the effect of CASK knockdown was first observed. A delayed response to CASK knockdown in synapse formation is consistent with our previous observation that the PDZ binding of syndecan-2 is not required for filopodia formation, the initial stage of spine formation, but is essential for transformation from filopodia to spines, the stage of spine maturation (Lin et al., 2007). It is very likely that CASK is mainly involved in the maturation or stabilization of dendritic spines by cross-linking adhesion molecules and the actin cytoskeleton. Consistent with this idea, overexpression of CASK in cultured hippocampal neurons increased the spine number but did not further enlarge the spine heads. It is possible that CASK stabilizes the labile spines and therefore increases the total spine number.

SUMOylation is an important posttranslational modification that modulates protein–protein interaction, subcellular distribution, and function of its target proteins. Recently, SUMOylation has been shown to regulate synapse function and formation (Martin et al., 2007). Kainate stimulation triggers SUMOylation of the kainate-sensitive glutamate receptor 6 and thus regulates endocytosis of glutamate receptor 6 (Martin et al., 2007). Kainate receptor–mediated excitatory postsynaptic currents are therefore decreased (Martin et al., 2007). Myocyte enhancer factor 2 (MEF2), a family of neuronal activity– and calcium-dependent transcription factors, is also regulated by SUMO conjugation.

SUMOylation at residue K403 of MEF2A promotes dendritic claw differentiation of cerebellar granule cells (Shalizi et al., 2006). MEF2 may control the expression of *arc* and *synGAP* genes and therefore regulate synapse formation (Flavell et al., 2006). Here, our data suggest another mechanism underlying SUMOylation regulation of synapse formation. SUMOylation of CASK modulates the interaction between CASK and protein 4.1, which may therefore down-regulate the association between CASK and the actin cytoskeleton. Although SUMOylated CASK proteins were still localized at synapses, they did not appear to be associated with the synaptic membrane. Instead, they were mainly present in the synaptic cytosol. Because overexpression of C-SUMO1-CASK impairs dendritic spine morphology, it suggests that SUMO1 conjugation leads to dissociation of CASK from postsynaptic plasma membrane. It may therefore uncouple adhesion molecules and actin cytoskeleton and destabilize dendritic spines.

In conclusion, our studies provide evidence that in addition to a presynaptic mechanism, CASK regulates synaptogenesis postsynaptically. CASK may link transmembrane adhesion molecules with actin cytoskeleton and therefore stabilize or maintain dendritic spine morphology. SUMOylation of CASK modulates the interaction between CASK and protein 4.1 and contributes to spinogenesis.

Materials and methods

Antibodies

CASK and PSD-95 monoclonal antibodies are available from Millipore. CASK rabbit polyclonal antibody was obtained from Santa Cruz Biotechnology, Inc. Myc tag monoclonal antibody 9B11 is available from Cell Signaling Technology. HA tag mouse monoclonal antibody 12CA5 and rabbit polyclonal antibody were purchased from Roche and Santa Cruz Biotechnology, Inc., respectively. FLAG tag M2 and β-tubulin monoclonal antibodies are available from Sigma-Aldrich. GFP rabbit polyclonal antibody was purchased from Invitrogen. Rabbit polyclonal and mouse monoclonal antibodies against SUMO1 were purchased from Invitrogen and Santa Cruz Biotechnology, Inc., respectively. Goat polyclonal antibody against Bassoon was purchased from Santa Cruz Biotechnology, Inc. SAP-97 antibody was a gift from M. Sheng (Howard Hughes Medical Institute, Massachusetts Institute of Technology, Cambridge, MA).

Plasmid construction

CASK shRNA construct in vector SM2c, which encodes a hairpin loop RNA corresponding to nt 784–804 of the rat CASK gene, was purchased from Open Biosystems. Myc-tagged CASK mutant resistant to CASK shRNA was mutated at residues 786, 789, and 792 of rat CASK by the QuikChange XL Site-Directed Mutagenesis kit (Stratagene). Plasmid expressing the HA-tagged PDZ domain was constructed by inserting the PDZ domain (residues 483–568 of rat CASK) into vector GW1-HA. CASK mutant lacking the protein 4.1–binding domain was constructed by inverted PCR using a pair of primers (5′-GCTTAATTAAGTACAAAGATAAATATTTGGC-3′ and 5′-CCTTAATTAAACAGCTGGCCTGCTGCTCTTG-3′). The PacI site was incorporated into the primers for cloning purposes. Amino acid residues 687–695 of rat CASK were thus replaced by Leu-Ile-Lys. For constructing the CASK K648R and K679R mutants, site-directed mutagenesis was performed with the QuikChange XL system using the primers 5′-CTGGTGGCAGGGTAGACTGGAAAACTCC-3′ and 5′-GAGGTTTTCCAGTCTACCCTGCCACCAG-3′ as well as 5′-CCATGGAGAAGACCAGACAAGAGCAGCAGGCCAG-3′ and 5′-CTGGCCTGCTGCTCTTGTCTGGTCTTCTCCATGG-3′, respectively; the underlined bases indicate the mutated sites. For construction of the syndecan-2 C-terminal fusion (synd-2C), GFP cDNA was first PCR amplified and subcloned into the vector GW1-myr-HA between the KpnI and BglII sites to yield the construct GFP/GW1-myr-HA. The fragment containing the last 36 residues of rat syndecan-2 was then subcloned into the BglII and EcoRI sites of GFP/GW1-myr-HA. Consequently, the GFP-Synd-2C/GW1-myr-HA construct expresses a HA and GFP double-tagged syndecan-2 C-terminal fusion. Plasmids for EGFP-actin and EGFP were purchased from Invitrogen.

Myc-SUMO1 expression plasmid was constructed by insertion of the SUMO1 fragment into a GW1 plasmid with the Myc cassette followed by RT-PCR amplification of SUMO1 cDNA from mouse brain RNA. The sequences of primers for amplifying SUMO1 were 5′-GCAACCCGGGTGTCTGACCAGGAGGCAAAACCTTC-3′ and 5′-CGAAGGTACCCTAAACCGTCGAGTGACCCCCCGT-3′; the underlined bases indicate the cloning sites XmaI and KpnI. For the EGFP-SUMO1 construct, SUMO1 cDNA flanked by XhoI sites was inserted into pEGFP-C1 plasmid. The sequences of primers for amplified SUMO1 were 5′-CCGTCTCGAGCTATGTCTGACCAGGAGGCAAAAC-3′ and 5′-CCGTCTCGAGCTAAACCGTCAGGTGACCCCCCG-3′; the underlined bases indicate the XhoI sites. The expressed sequence tag clone of protein 4.1N (Invitrogen) was used as the template for PCR amplification of protein 4.1N cDNA. The protein 4.1N cDNA was amplified using the primers 5′-ATCGGAATTCCATGACAACAGAGACAGGT-3′ and 5′-ACCGGGATCTCTAGGATTCCTGTGGCTTC-3′ and was ligated into pFLAG-CMV-2 plasmid flanked by BamHI and EcoRI. For the construction of C- and CN-SUMO1-CASK, the three primers PCR strategy was applied. The pairs of primers used for construction of C- and CN-SUMO1-CASK were as follows: (1) for the fragment in which SUMO1 was deleted in the C-terminal GG region, 5′-ATGTCTGACCAGGAGGCAAAACCTTC-3′ and 5′-CGTTTGTTCCTGATAAACTTCAATC-3′; (2) for the full-length CASK fragment, 5′-ATGGCCGACGACGACGTGCTGTTCG-3′ and 5′-ATAGACCCAGGAGACCGGGACCCAC-3′; and (3) for the C-SUMO1-CASK fragment, 5′-GCAACCCGGGGCCGACGACGACGTGCTGTTCGAGG-3′, 5′-GCGAGAATTCTACGTTTGTTCCTGATAAACTTCAATC-3′, and 5′-GTCCCGGTCTCCTGGGTCTATATGTCTGACCAGGAGGCAAAAC-3′. The CN-SUMO1-CASK clone was constructed by ligating the C-SUMO1-CASK fragment into the GW-Myc-SUMO1 plasmid.

Animals and housing

All animal experiments were performed with the approval and in strict accordance with the guidelines of the Academia Sinica Institutional Animal Care and Utilization Committee and the Republic of China Council of Agriculture Guidebook for the Care and Use of Laboratory Animals. Pregnant rats were housed individually and killed by CO_2 inhalation. All efforts were made to minimize animal suffering and to reduce the number of animals required.

Cultured hippocampal neurons and immunofluorescence analysis

Hippocampal neurons from embryonic day 18–19 rat embryos were cultured as described previously (Lin et al., 2006; Lin et al., 2007). For immunofluorescence analysis, cells were seeded on coverslips (18 mm in diameter and 0.12–0.17 mm in thickness) coated with poly-L-lysine. Calcium phosphate precipitation was used to deliver plasmid DNA into neurons. 2–7 d after transfection, cells were fixed with 4% PFA and 4% sucrose in PBS. After permeabilizing with cold methanol (−20°C) for 15 min at −20°C, neurons were blocked by incubating with 10% BSA for 2 h. The cells were probed by specific first antibodies diluted in PBS (5% BSA) at 4°C overnight. After several washes, the AlexaFluor488-, 555-, or 647-conjugated secondary antibody (Invitrogen) was added and incubated for 2 h. The processed cells were embedded in Vectashield mounting medium (Vector Laboratories) for image acquisition. Samples were then analyzed at room temperature with either a fluorescence microscope (DM RE; Leica) with a PLAPO 63× 1.32 NA oil objective lens or a confocal microscope (LSM510META; Carl Zeiss, Inc.) with a Plan-Apochromat 63× 1.25 NA oil objective lens. For regular fluorescence microscopy, images were acquired with a cooled CCD camera (RTE/CCD-1300-Y/HS; Roper Scientific) operated using MetaMorph software (MDS Analytical Technologies). For confocal microscopy, the images were acquired using a laser-scanning microscope (LSM510META system; Carl Zeiss, Inc.) with a resolution of 1,024 × 1,024 pixels. Results were then processed for publication using Photoshop software (Adobe) with minimal adjustment of brightness or contrast applied to the whole images.

Neuronal treatments

Neurons at 17–18 DIV were incubated overnight in neurobasal culture medium containing 1 µM TTX. Before high KCl treatment, medium containing TTX was removed, followed by three washes in fresh neurobasal culture medium, before cells were incubated in neurobasal culture medium for 1.5 h. For high K^+ stimulation, 1 ml Tyrode-HK solution (25 mM Hepes, 62.5 mM NaCl, 60 mM KCl, 2 mM $CaCl_2$, and 2 mM MgCl, pH 7.4) was added to the neurons at 37°C with 5% CO_2 for 3 min. The Tyrode-HK solution was then removed, and the neurons were washed three times in neurobasal culture medium. After the wash, the high K^+-treated neurons were incubated

in fresh neurobasal culture medium for another 20–40 min before fixing for immunostaining.

Analysis of dendritic spine formation and spine puncta

For dendritic spine analysis, Z series confocal images were collected as described in the previous section. Each image consisted of 7–12 sections spaced 0.5 µm apart. The data were collected from two to three independent culture preparations. Morphometric measurement was performed with MetaMorph software. Images were zoomed to three times magnification, and the number of spines and each individual spine present on the dendrites (along 20 µm of each dendrite starting from a point 20 µm away from the soma) was manually counted and traced. The maximum length from the tip of the spine to dendritic shaft and head width of each spine was manually measured by region measurement. The data were then exported to Excel (Microsoft) for further analysis. The significance of differences between treatments was determined by KS test based on the D and corresponding p-values. For KS tests, the original raw data were used. For display purposes, the data for the graphs of cumulative probability distributions were binned. The mean and standard error of each group are also shown in the figures.

For synaptic puncta analysis, the number of puncta (along 20 µm of each dendrite starting from a point 20 µm away from the soma) was manually counted, and each individual punctum present on the dendrites was traced by MetaMorph software version 7.1.4.0. The data were then exported to Excel for further analysis. Data were expressed as the mean values ± SEM. Intergroup comparisons were made with an unpaired *t* test using SPSS software (SPSS, Inc.), and $P < 0.05$ indicated statistically significant differences.

Subcellular fractionation

A mouse brain was rapidly removed from the skull and homogenized with 20 strokes of a Teflon glass homogenizer in 2 ml of ice-cold lysis buffer containing 320 mM sucrose, 4 mM Hepes, pH 7.4, 1 mM EGTA, and protease inhibitor mix (Roche). Homogenates were centrifuged at 700 *g* for 10 min at 4°C. The supernatant (S1) was centrifuged again at 9,250 *g* for 15 min to obtain synaptosome fraction (P2). For separation of synaptic cytosol containing vesicles (LS1) and synaptic membrane (LP1), the pellet (P2) was hypoosmotically lysed and centrifuged at 25,000 *g* for 20 min. LS1 was further centrifuged at 100,000 *g* for 120 min to obtain the crude synaptic vesicle (LP2) and synaptic cytosol (LS2) fractions. P3 and S3 were obtained by centrifugation of S2 at 100,000 *g* for 2 h. Protein concentration was determined by a Bradford protein assay (Bio-Rad Laboratories).

Transfection, immunoblotting, and immunoprecipitation

Transfection conditions for HEK and COS cells were the same as those described previously (Hsueh and Sheng, 1999b). For immunoblotting analysis, 1 d after transfection, cells were washed with PBS twice and lysed directly using SDS sample buffer with protease inhibitor mixture. After boiling for 5 min, the total cell lysates were then separated by SDS-PAGE and analyzed by immunoblotting.

To perform immunoprecipitation of CASK, transfected COS cells were first washed with PBS. Immunoprecipitation lysis buffer without detergent (50 mM Tris–HCl, pH 7.4, 100 mM KCl, 0.1 mM DTT, and protease inhibitor mixture) was then added for cell harvest. After sonication for 10 s, the cell lysates were treated with Triton X-100 (final 1% concentration) and incubated at 4°C for 30 min. The lysates were centrifuged at 13,000 *g* for 30 min to remove the insoluble fraction, and protein concentrations were then determined using a bicinchoninic acid protein assay kit (Thermo Fisher Scientific). 1-mg aliquots of solubilized protein extracts was mixed with 30 µl CASK monoclonal antibody–conjugated beads (50% slurry) and incubated at 4°C overnight. Beads were then washed in lysis buffer containing 1% Triton X-100 and 5 mM EDTA, in lysis buffer containing 1% Triton X-100, and in PBS, three times for each buffer.

For coimmunoprecipitation of CASK and protein 4.1N, extracts were prepared for CASK immunoprecipitation except that the concentration of Triton X-100 was decreased to 0.5%. 0.5-mg aliquots of protein extracts was mixed with 30 µl M2-conjugated beads or 30 µl mouse antiactin antibody–conjugated beads (50% slurry) and incubated at 4°C overnight. Beads were then washed in lysis buffer containing 1% Triton X-100 and 5 mM EDTA, in lysis buffer containing 1% Triton X-100, and in PBS, three times for each buffer. One fifth of immunoprecipitation products was separated by regular SDS-PAGE on 8 or 10% gels, with 10 µg of protein loaded as input comparison. The separated proteins were transferred to polyvinylidene difluoride membranes and analyzed by immunoblotting.

Online supplemental material

Fig. S1 shows the knockdown effect of CASK shRNA after 2 d of incubation. Fig. S2 shows the time course of CASK knockdown in cultured neurons. Fig. S3 shows the distribution of wild-type CASK and C-SUMO1-CASK in cultured hippocampal neurons. Online supplemental material is available at http://www.jcb.org/cgi/content/full/jcb.200712094/DC1.

We thank Dr. Morgan Sheng for SAP97 antibody, Sue-Ping Lee for technical assistance with confocal analysis, and Dr. Harry Wilson for English language editing.

This work was supported by grants from Academia Sinica, the National Science Council (NSC 96-2321-B-001-005 to Y.-P. Hsueh), and the National Health Research Institute (NHRI-EX97-9403NI to Y.-P. Hsueh).

Submitted: 18 December 2007
Accepted: 9 June 2008

References

Alkuraya, F.S., I. Saadi, J.J. Lund, A. Turbe-Doan, C.C. Morton, and R.L. Maas. 2006. SUMO1 haploinsufficiency leads to cleft lip and palate. *Science.* 313:1751.

Atasoy, D., S. Schoch, A. Ho, K.A. Nadasy, X. Liu, W. Zhang, K. Mukherjee, E.D. Nosyreva, R. Fernandez-Chacon, M. Missler, et al. 2007. Deletion of CASK in mice is lethal and impairs synaptic function. *Proc. Natl. Acad. Sci. USA.* 104:2525–2530.

Biederer, T., and T.C. Sudhof. 2001. CASK and protein 4.1 support F-actin nucleation on neurexins. *J. Biol. Chem.* 276:47869–47876.

Biederer, T., Y. Sara, M. Mozhayeva, D. Atasoy, X. Liu, E.T. Kavalali, and T.C. Sudhof. 2002. SynCAM, a synaptic adhesion molecule that drives synapse assembly. *Science.* 297:1525–1531.

Borg, J.P., S.W. Straight, S.M. Kaech, M. de Taddeo-Borg, D.E. Kroon, D. Karnak, R.S. Turner, S.K. Kim, and B. Margolis. 1998. Identification of an evolutionarily conserved heterotrimeric protein complex involved in protein targeting. *J. Biol. Chem.* 273:31633–31636.

Bretscher, A., K. Edwards, and R.G. Fehon. 2002. ERM proteins and merlin: integrators at the cell cortex. *Nat. Rev. Mol. Cell Biol.* 3:586–599.

Butz, S., M. Okamoto, and T.C. Sudhof. 1998. A tripartite protein complex with the potential to couple synaptic vesicle exocytosis to cell adhesion in brain. *Cell.* 94:773–782.

Cohen, A.R., D.F. Woods, S.M. Marfatia, Z. Walther, A.H. Chishti, J.M. Anderson, and D.F. Wood. 1998. Human CASK/LIN-2 binds syndecan-2 and protein 4.1 and localizes to the basolateral membrane of epithelial cells. *J. Cell Biol.* 142:129–138.

Elias, G.M., L. Funke, V. Stein, S.G. Grant, D.S. Bredt, and R.A. Nicoll. 2006. Synapse-specific and developmentally regulated targeting of AMPA receptors by a family of MAGUK scaffolding proteins. *Neuron.* 52:307–320.

Ethell, I.M., and Y. Yamaguchi. 1999. Cell surface heparan sulfate proteoglycan syndecan-2 induces the maturation of dendritic spines in rat hippocampal neurons. *J. Cell Biol.* 144:575–586.

Ethell, I.M., K. Hagihara, Y. Miura, F. Irie, and Y. Yamaguchi. 2000. Synbindin, a novel syndecan-2-binding protein in neuronal dendritic spines. *J. Cell Biol.* 151:53–68.

Flavell, S.W., C.W. Cowan, T.K. Kim, P.L. Greer, Y. Lin, S. Paradis, E.C. Griffith, L.S. Hu, C. Chen, and M.E. Greenberg. 2006. Activity-dependent regulation of MEF2 transcription factors suppresses excitatory synapse number. *Science.* 311:1008–1012.

Gao, Y., M. Li, W. Chen, and M. Simons. 2000. Synectin, syndecan-4 cytoplasmic domain binding PDZ protein, inhibits cell migration. *J. Cell. Physiol.* 184:373–379.

Grootjans, J.J., P. Zimmermann, G. Reekmans, A. Smets, G. Degeest, J. Durr, and G. David. 1997. Syntenin, a PDZ protein that binds syndecan cytoplasmic domains. *Proc. Natl. Acad. Sci. USA.* 94:13683–13688.

Hoover, K.B., and P.J. Bryant. 2000. The genetics of the protein 4.1 family: organizers of the membrane and cytoskeleton. *Curr. Opin. Cell Biol.* 12:229–234.

Hsueh, Y.P. 2006. The role of the MAGUK protein CASK in neural development and synaptic function. *Curr. Med. Chem.* 13:1915–1927.

Hsueh, Y.P., and M. Sheng. 1999a. Regulated expression and subcellular localization of syndecan heparan sulfate proteoglycans and the syndecan-binding protein CASK/LIN-2 during rat brain development. *J. Neurosci.* 19:7415–7425.

Hsueh, Y.P., and M. Sheng. 1999b. Requirement of N-terminal cysteines of PSD-95 for PSD-95 multimerization and ternary complex formation, but not for binding to potassium channel Kv1.4. *J. Biol. Chem.* 274:532–536.

Hsueh, Y.P., F.C. Yang, V. Kharazia, S. Naisbitt, A.R. Cohen, R.J. Weinberg, and M. Sheng. 1998. Direct interaction of CASK/LIN-2 and syndecan heparan

sulfate proteoglycan and their overlapping distribution in neuronal synapses. *J. Cell Biol.* 142:139–151.

Hsueh, Y.P., T.F. Wang, F.C. Yang, and M. Sheng. 2000. Nuclear translocation and transcription regulation by the membrane-associated guanylate kinase CASK/LIN-2. *Nature.* 404:298–302.

Irie, M., Y. Hata, M. Takeuchi, K. Ichtchenko, A. Toyoda, K. Hirao, Y. Takai, T.W. Rosahl, and T.C. Sudhof. 1997. Binding of neuroligins to PSD-95. *Science.* 277:1511–1515.

Jo, K., R. Derin, M. Li, and D.S. Bredt. 1999. Characterization of MALS/Velis-1, -2, and -3: a family of mammalian LIN-7 homologs enriched at brain synapses in association with the postsynaptic density-95/NMDA receptor postsynaptic complex. *J. Neurosci.* 19:4189–4199.

Kaech, S.M., C.W. Whitfield, and S.K. Kim. 1998. The LIN-2/LIN-7/LIN-10 complex mediates basolateral membrane localization of the *C. elegans* EGF receptor LET-23 in vulval epithelial cells. *Cell.* 94:761–771.

Kim, S., A. Burette, H.S. Chung, S.K. Kwon, J. Woo, H.W. Lee, K. Kim, H. Kim, R.J. Weinberg, and E. Kim. 2006. NGL family PSD-95-interacting adhesion molecules regulate excitatory synapse formation. *Nat. Neurosci.* 9:1294–1301.

Laverty, H.G., and J.B. Wilson. 1998. Murine CASK is disrupted in a sex-linked cleft palate mouse mutant. *Genomics.* 53:29–41.

Lin, C.W., T.N. Huang, G.S. Wang, T.Y. Kuo, T.Y. Yen, and Y.P. Hsueh. 2006. Neural activity- and development-dependent expression and distribution of CASK interacting nucleosome assembly protein in mouse brain. *J. Comp. Neurol.* 494:606–619.

Lin, Y.-L., Y.-T. Lei, C.-J. Hong, and Y.P. Hsueh. 2007. Syndecan-2 induces filopodia formation via the neurofibromin-PKA-Ena/VASP pathway. *J. Cell Biol.* 177:829–841.

Martin, S., A. Nishimune, J.R. Mellor, and J.M. Henley. 2007. SUMOylation regulates kainate-receptor-mediated synaptic transmission. *Nature.* 447:321–325.

Maximov, A., and I. Bezprozvanny. 2002. Synaptic targeting of N-type calcium channels in hippocampal neurons. *J. Neurosci.* 22:6939–6952.

Migaud, M., P. Charlesworth, M. Dempster, L.C. Webster, A.M. Watabe, M. Makhinson, Y. He, M.F. Ramsay, R.G. Morris, J.H. Morrison, et al. 1998. Enhanced long-term potentiation and impaired learning in mice with mutant postsynaptic density-95 protein. *Nature.* 396:433–439.

Nam, C.I., and L. Chen. 2005. Postsynaptic assembly induced by neurexin-neuroligin interaction and neurotransmitter. *Proc. Natl. Acad. Sci. USA.* 102:6137–6142.

Olsen, O., K.A. Moore, M. Fukata, T. Kazuta, J.C. Trinidad, F.W. Kauer, M. Streuli, H. Misawa, A.L. Burlingame, R.A. Nicoll, and D.S. Bredt. 2005. Neurotransmitter release regulated by a MALS-liprin-alpha presynaptic complex. *J. Cell Biol.* 170:1127–1134.

Pichler, A., and F. Melchior. 2002. Ubiquitin-related modifier SUMO1 and nucleocytoplasmic transport. *Traffic.* 3:381–387.

Samuels, B.A., Y.P. Hsueh, T. Shu, H. Liang, H.C. Tseng, C.J. Hong, S.C. Su, J. Volker, R.L. Neve, D.T. Yue, and L.H. Tsai. 2007. Cdk5 promotes synaptogenesis by regulating the subcellular distribution of the MAGUK family member CASK. *Neuron.* 56:823–837.

Setou, M., T. Nakagawa, D.H. Seog, and N. Hirokawa. 2000. Kinesin superfamily motor protein KIF17 and mLin-10 in NMDA receptor-containing vesicle transport. *Science.* 288:1796–1802.

Shalizi, A., B. Gaudilliere, Z. Yuan, J. Stegmuller, T. Shirogane, Q. Ge, Y. Tan, B. Schulman, J.W. Harper, and A. Bonni. 2006. A calcium-regulated MEF2 sumoylation switch controls postsynaptic differentiation. *Science.* 311:1012–1017.

Shalizi, A., P.M. Bilimoria, J. Stegmuller, B. Gaudilliere, Y. Yang, K. Shuai, and A. Bonni. 2007. PIASx is a MEF2 SUMO E3 ligase that promotes postsynaptic dendritic morphogenesis. *J. Neurosci.* 27:10037–10046.

Sytnyk, V., I. Leshchyns'ka, A.G. Nikonenko, and M. Schachner. 2006. NCAM promotes assembly and activity-dependent remodeling of the postsynaptic signaling complex. *J. Cell Biol.* 174:1071–1085.

van Niekerk, E.A., D.E. Willis, J.H. Chang, K. Reumann, T. Heise, and J.L. Twiss. 2007. Sumoylation in axons triggers retrograde transport of the RNA-binding protein La. *Proc. Natl. Acad. Sci. USA.* 104:12913–12918.

Varoqueaux, F., G. Aramuni, R.L. Rawson, R. Mohrmann, M. Missler, K. Gottmann, W. Zhang, T.C. Sudhof, and N. Brose. 2006. Neuroligins determine synapse maturation and function. *Neuron.* 51:741–754.

Wilson, V.G., and D. Rangasamy. 2001. Intracellular targeting of proteins by sumoylation. *Exp. Cell Res.* 271:57–65.

Wong, R.W., M. Setou, J. Teng, Y. Takei, and N. Hirokawa. 2002. Overexpression of motor protein KIF17 enhances spatial and working memory in transgenic mice. *Proc. Natl. Acad. Sci. USA.* 99:14500–14505.